J|A|C|S
ARTICLES

Published on Web 06/07/2008

Cooperativity and Tunable Excited State Deactivation: Modular Self-Assembly of Depsipeptide Dendrons on a Hamilton Receptor Modified Porphyrin Platform

Jan-Frederik Gnichwitz,[†] Mateusz Wielopolski,[‡] Kristine Hartnagel,[†] Uwe Hartnagel,[†] Dirk M. Guldi,*[,‡] and Andreas Hirsch*[,†]

Department of Chemistry and Pharmacy, and Interdisciplinary Center of Molecular Materials (ICMM), Friedrich-Alexander-Universität Erlangen-Nürnberg, Henkestrasse 42, 91054-Erlangen, Germany and Department of Chemistry and Pharmacy, and Interdisciplinary Center of Molecular Materials (ICMM), Friedrich-Alexander-Universität Erlangen-Nürnberg, Egerlandstrasse 3, 91058-Erlangen, Germany

Received March 11, 2008; E-mail: dirk.guldi@chemie.uni-erlangen.de; andreas.hirsch@chemie.uni-erlangen.de

Abstract: A series of novel supramolecular architectures were built around a tin tetraphenyl porphyrin platform **6**—functionalized by a 2-fold 1-ethyl-3-3-(3-dimethylaminopropyl)carbodiimide (EDC) promoted condensation reaction—and chiral depsipeptide dendrons of different generations **1**—**4**. Here, implementation of a Hamilton receptor provided the necessary means to keep the constituents together via strong hydrogen bonding. Characterization of all architectures has been performed, including **4** which is the fourth generation, on the basis of NMR and photophysical methods. In particular, several titration experiments were conducted suggesting positive cooperativity, an assessment that is based on association constants that tend to be higher for the second binding step than for the first step. Importantly, molecular modeling calculations reveal a significant deaggregation of the intermolecular network of **6** during the course of the first binding step. As a consequence, an improved accessibility of the second Hamilton receptor unit in **6** emerges and, in turn, facilitates the higher association constants. The features of the equilibrium, that is, the dynamic exchange of depsipeptide dendrons **1**—**4** with fullerene **5**, was tested in photophysical reference experiments. These steady-state and time-resolved measurements showed the tunable excited-state deactivations of these complexes upon photoexcitation.

Introduction

Until now, nature provides the most efficient pathways for solar energy conversion. For example, natural photoactive centers transform solar light into useful chemical energy in quantum yields close to unity. Generally speaking, these energy conversion processes involve three primary photochemical events: light absorption, excitation energy transduction, and photoinduced electron or energy transfer, respectively.[1,2] Therefore, one of the most exciting topics in current research is to further advance the comprehension and optimization of each of these key steps, which are all essential for developing photosynthetic systems that are capable of efficient solar-energy conversion.

Porphyrins and other closely related tetrapyrrolic pigments are widely spread in nature and play very important roles in various biological processes. Owing to their macrocylic molecular architectures, these molecules provide excellent platforms for light-harvesting and electron/energy-transfer performances.[3] The implementation of these features into practical applications requires, however, adapting a coherent strategy, via molecular engineering, to reconstitute the natural biological environment.

The unique redox and structural properties of C_{60} provide valuable incentives for their use as electron accepting building blocks.[4,5] Remarkable is that when integrating C_{60}, for example, together with porphyrins into electron donor—acceptor arrays, C_{60} commonly retains its characteristic low reorganization energy in electron transfer reactions. Consequently, porphyrin-C_{60} arrays are ideally suited to generate long-lived radical ion pair states in high yields.[6] Up to date, most porphyrin-C_{60} systems are, nevertheless, based on a covalent linkage. The role

[†] Friedrich-Alexander-Universität Erlangen-Nürnberg, Henkestrasse 42.
[‡] Friedrich-Alexander-Universität Erlangen-Nürnberg, Egerlandstrasse 3.

(1) (a) Feher, G.; Allen, J. P.; Okamura, M. Y.; Rees, D. C. *Nature* **1989**, *339*, 111. (b) Deisenhofer, J.; Michel, H. *Angew. Chem.* **1989**, *101*, 872; *Angew. Chem., Int. Ed. Engl.* **1989**, *28*, 829. (c) Huber, R. *Angew. Chem.* **1989**, *101*, 849; *Angew. Chem., Int. Ed. Engl.* **1989**, *28*, 848. (d) *The Photosynthetic Reaction Center*; Deisenhoifer, J., Norris, J. R., Eds.; Academic Press: New York, 1993. (e) *Molecular Mechanisms of Photosynthesis*; Blankenship, R. E., Ed.; Blackwell Science: 2002.

(2) (a) Balzani, V.; Scandola, F. *Supramolecular Photochemistry*; Ellis Horwood: Chichester, U.K., 1991; pp 161—196, 355—394. (b) Turro, N. J. *Modern Molecular Photochemistry*; University Science Books: Mill Valley, CA, 1991; pp 321—361. (c) Speiser, S. *Chem. Rev.* **1996**, *96*, 1953.

(3) *The Porphyrin Handbook*; Kadish, K. M., Smith, K. M., Guillard, R., Eds.; Academic Press: San Diego, 2003.

(4) Echegoyen, L.; Echegoyen, L. E. *Acc. Chem. Res.* **1998**, *31*, 593.

(5) (a) *The Chemistry of the Fullerenes*; Hirsch, A., Ed.; Georg Thieme Verlag: Stuttgart, 1994. (b) Dresselhaus M. S.; Dresselhaus, G.; Eklund, P. C. *Science of Fullerenes and Carbon Nanotubes*; Academic Press: San Diego, 1996. (c) *Fullerenes: from Synthesis to Optoelectronic Properties*; Guldi, D. M., Martín, N., Eds.; Kluwer Academic Publishers: Dodrech, 2002.

played by the linker is not just structural, since its chemical nature governs the electronic communication between the terminal units (i.e., porphyrin and C_{60}). Another important feature of the spacer is its modular composition, which allows altering the separation without affecting the electronic nature of the connection.

Noncovalent electron donor−acceptor nanohybrids based on supramolecular interactions are rarely known.[7] To this end, we have published the synthesis of an electron-transfer system based on noncovalent electrostatic interactions between C_{60} and a porphyrin or cytochrome C complex. In the resulting coulomb complexes, the interactions between, for instance, the dendritic C_{60} oligocarboxylate and the octapyridinium porphyrin salt stem from the oppositely charged head groups of the two building blocks. This, in turn, provides sufficiently strong electronic couplings to power intrahybrid charge-separation processes.[8] With respect to photoinduced charge separation, this approach provides benefits for the successful fabrication of photovoltaic devices that perform efficiently on the basis of hierarchically ordering the individual building blocks, namely, donors and acceptors.

Among the many supramolecular binding motifs that are available, hydrogen bonding is considered as the structurally most potent one. We have already shown the enormous potential that rests on the highly directional self-assembly of porphyrin-C_{60} electron donor−acceptor hybrids via hydrogen bonding. In fact, our approach ensures (i) fine-tuning of the complexation strength, (ii) regulation of the electronic coupling and its impact on electron- and energy-transfer processes, and (iii) high solubility of the corresponding hybrid architectures.[9]

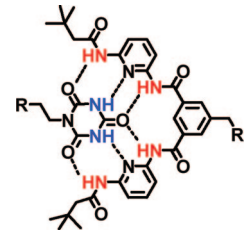

Figure 1. Schematic representation of the complementary hydrogen bonding motif of a cyanuric acid derivative and a Hamilton receptor.

Recently, we have introduced a series of first-, second-, and third-generation depsipeptide dendrons, including the all-*R* configured **1**−**3** that bear cyanuric acid moieties at their focal points.[10] Strong six-point hydrogen bonding ($K_a \approx 10^3-10^6$ M^{-1}) with, for example, complementary Hamilton receptors[11] (Figure 1) attached to a variety of molecular platforms renders these dendrons as excellent building blocks to achieve the facile construction of new functional supramolecular architectures.[10,12] These include self-assembled dendrimers involving porphyrins as electroactive components, which, except for the dendritic pocket receptors reported by Tsukube and co-workers,[13] are the first representatives of this hydrogen bonded class of compounds.[14] Covalent dendrimers with porphyrin cores, on the other hand, have been extensively investigated as intriguing mimics for globular heme proteins.[15]

The importance of noncovalent building principles in protein chemistry is undisputed and inspired us to develop *for the first time* a modular concept toward supramolecular heme-protein models. Key features are chromophoric and nonchromophoric depsidpeptide dendrons **1**−**5** as protein mimics, which are interchangeable at the tin-tetraphenyl-porphyrin (SnP) platform

(6) (a) Imahori, H.; Sakata, Y. *Adv. Mater.* **1997**, *9*, 537. (b) Prato, M. *J. Mater. Chem.* **1997**, *7*, 1097. (c) Martín, N.; Sánchez, L.; Illescas, B.; Pérez, I. *Chem. Rev.* **1998**, *98*, 2527. (d) Diederich, F.; Gómez-López, M. *Chem. Soc. Rev.* **1999**, *28*, 263. (e) Imahori, H.; Sakata, Y. *Eur. J. Org. Chem.* **1999**, 2445. (f) Guldi, D. M. *Chem. Commun.* **2000**, 321. (g) Guldi, D. M.; Prato, M. *Acc. Chem. Res.* **2000**, *33*, 695. (h) Reed, C. A.; Bolskar, R. D. *Chem. Rev.* **2000**, *100*, 1075. (i) Gust, D.; Moore, T. A.; Moore, A. L. *J. Photochem. Photobiol. B.* **2000**, *58*, 63. (j) Gust, D.; Moore, T. A.; Moore, A. L. *Acc. Chem. Res.* **2001**, *34*, 40. (k) Guldi, D. M. *Chem. Soc. Rev.* **2002**, *31*, 22. (l) Guldi, D. M.; Martín, N. *J. Mater. Chem* **2002**, *12*, 1978. (m) Meijer, M. D.; van Klink, G. P. M.; van Koten, G. *Coord. Chem. Rev.* **2002**, *230*, 141. (n) Guldi, D. M. *Pure Appl. Chem.* **2003**, *75*, 1069. (o) Imahori, H.; Mori, Y.; Matano, Y. *J. Photochem. Photobiol. C* **2003**, *4*, 51.

(7) (a) Fernández, G.; Pérez, E. M.; Sánchez, L.; Martín, N. *Angew. Chem.* **2008**, *120*, 1110; *Angew. Chem., Int. Ed.* **2008**, *47*, 1094. (b) Torres, T.; Gouloumis, A.; Sanchez-Garcia, D.; Jayawickramarajah, J.; Seitz, W.; Guldi, D. M.; Sessler, J. L. *Chem. Commun.* **2007**, 292. (c) McClenaghan, N. D.; Grote, Z.; Darriet, K.; Zimine, M.; Williams, R. M.; de Cola, L.; Bassani, D. M. *Org. Lett.* **2005**, *7*, 807. (d) Beckers, E. H. A.; Schenning, A. P. H. J.; van Hal, P. A.; El-ghayoury, A.; Sánchez, L.; Hummelen, J. C.; Meijer, E. W.; Janssen, R. A. J. *Chem. Commun.* **2002**, 2888. (e) Mateo-Alonso, A.; Sooambar, C.; Prato, M. C. R. *Chim.* **2006**, *9*, 944. (f) Eckart, J.-F.; Byrne, D.; Nicoud, J.-F.; Oswald, L.; Nierengarten, J.-F.; Numata, M.; Ikeda, A.; Shinaki, S.; Armaroli, N. *New. J. Chem.* **2000**, *24*, 749. (g) Diederich, F.; Kessinger, R. *Acc. Chem. Res.* **1999**, *32*, 537–545. (h) Spillmann, H.; Kiebele, A.; Stö hr, M.; Jung, T. A.; Bonifazi, D.; Cheng, F. Y.; Diederich, F. *Adv. Mater.* **2006**, *18*, 275. (i) Bonifazi, D.; Accorsi, G.; Armaroli, N.; Song, F. Y.; Palkar, A.; Echegoyen, L.; Scholl, M.; Seiler, P.; Jaun, P.; Diederich, F. *Helv. Chim. Acta* **2005**, *88*, 1839. (j) Bonifazi, D.; Spillmann, H.; Kiebele, A.; de Wild, M.; Seiler, P.; Cheng, F. Y.; Güntherodt, H. J.; Jung, T.; Diederich, F. *Angew. Chem.* **2004**, *116*, 4863; *Angew. Chem., Int. Ed.* **2004**, *43*, 4759. (k) Bonifazi, D.; Diederich, F. *Chem. Commun.* **2002**, 2178.

(8) (a) Guldi, D. M.; Zilbermann, I.; Anderson, G.; Li, A.; Balbinot, D.; Jux, N.; Hatzimarinaki, M.; Hirsch, A.; Prato, M. *Chem. Commun.* **2004**, *6*, 726. (b) Balbinot, D.; Atalick, S.; Guldi, D. M.; Hatzimarinaki, M.; Hirsch, A.; Jux, N. *J. Phys. Chem. B* **2003**, *107*, 13273. (c) Hartnagel, U.; Balbinot, D.; Jux, N.; Hirsch, A. *Org. Biomol. Chem.* **2006**, *4*, 1785.

(9) (a) Wessendorf, F.; Gnichwitz, J.-F.; Sarova, G. H.; Hager, K.; Hartnagel, U.; Guldi, D. M.; Hirsch, A. *J. Am. Chem. Soc.* **2007**, *129*, 16057. (b) Sanchez, L.; Sierra, M.; Martin, N.; Myles, A. J.; Dale, T. J.; Rebek, Jr, J.; Seitz, W.; Guldi, D. M. *Angew. Chem.* **2006**, *118*, 4753; *Angew. Chem., Int. Ed.* **2006**, *45*, 4637. (c) D'Souza, F.; El-Khouly, M. E.; Gadde, S.; Zandler, M. E.; McCarty, A. L.; Araki, Y.; Ito, O. *Tetrahedron* **2005**, *62*, 1967. (d) Guldi, D. M. *Chem. Commun.* **2000**, *5*, 321. (e) Sessler, J. S.; Wang, B.; Springs, S. L.; Brown C. T. In *Comprehensive Supramolecular Chemistry*; Atwood, J. L., Davies, J. E. D., MacNicol, D. D., Vögtle, F., Eds.; Pergamon: New York, 1996; Chapter 9. (f) Piotrowiak, P. *Chem. Soc. Rev.* **1999**, *28*, 143.

(10) (a) Hager, K.; Franz, A.; Hirsch, A. *Chem.—Eur. J.* **2006**, *12*, 2663. (b) Maurer, K.; Hager, K.; Hirsch, A. *Eur. J. Org. Chem.* **2006**, *15*, 3338. (c) Hager, K.; Hartnagel, U.; Hirsch, A. *Eur. J. Org. Chem.* **2007**, *12*, 1942.

(11) Chang, S. K.; Hamilton, A. D. *J. Am. Chem. Soc.* **1988**, *110*, 1318.

(12) Berl, V.; Schmutz, M.; Krische, M. J.; Khoury, R. G.; Lehn, J. M. *Chem.—Eur. J.* **2002**, *8*, 1227.

(13) Shinoda, S.; Ohashi, M.; Tsukube, H. *Chem.—Eur. J.* **2007**, *13*, 81.

(14) For systems involving coordinative complexation of dendritic ligand to a porphyrin platform, see: Tomoyose, Y.; Jiang, D.-L.; Jin, R.-H.; Aida, T.; Yamashita, T.; Horie, K.; Yashima, E.; Okamoto, Y. *Macromolecules* **1996**, *29*, 5236.

(15) (a) Felber, B.; Diederich, F. *Helv. Chim. Acta* **2005**, *88*, 120. (b) Collmann, J. P.; Boulatov, R.; Sunderland, C. J.; Fu, L. *Chem. Rev.* **2004**, *104*, 561. (c) Weyermann, P.; Diederich, F. *Helv. Chim. Acta* **2002**, *85*, 599. (d) Matos, M. S.; Hofkens, J.; Verheijen, W.; De Schryver, F. C.; Hecht, S.; Pollak, K. W.; Fréchet, J. M. J.; Forier, B.; Dehaen, W. *Macromolecules* **2000**, *33*, 2967. (e) Weyermann, P.; Gisselbrecht, J.-P.; Boudon, C.; Diederich, F.; Gross, M. *Angew. Chem.* **1999**, *111*, 3400; *Angew. Chem., Int. Ed. Engl.* **1999**, *38*, 3215. (f) Pollak, K. W.; Leon, J. W.; Fréchet, J. M. J.; Maskus, M.; Abruña, H. D. *Chem. Mater.* **1998**, *10*, 30. (g) Dandliker, P. J.; Diederich, F.; Gross, M.; Knobler, C. B.; Louati, A.; Sanford, E. *Angew. Chem.* **1994**, *106*, 1821; *Angew. Chem., Int. Ed. Engl.* **1994**, *33*, 1739.

Chart 1

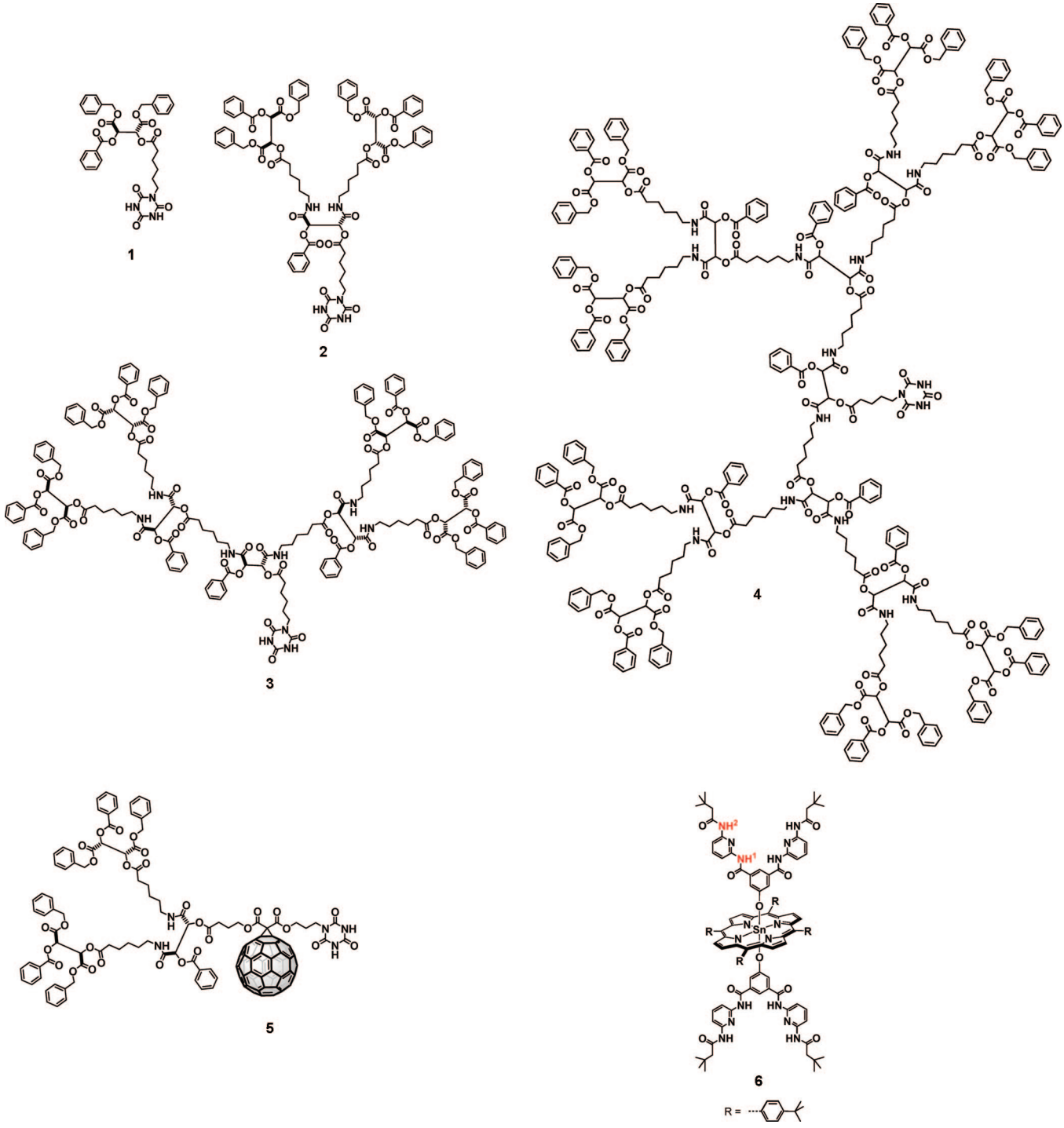

(**6**) (Chart 1). The latter contains two axial Hamilton receptors. This scenario allows investigating ligand dependent binding cooperativity and successive fluorescence quenching via energy transfer between porphyrins and fullerenes in the corresponding 1:2 complexes.

Results and Discussion

In the current work, we wish to introduce as a complement to the series of recently synthesized depsipeptide dendrons **1**−**3** and **5**[10] the fourth generation representative **4**. The enantiomerically pure dendron **4** contains 30 stereogenic centers with all *R*-configuration and is the largest building block known to date within the context of constructing chiral self-assembled dendrimers. The key synthetic step is the 2-fold peptide coupling of a tartaric acid core to a third generation amine precursor (Scheme 1).

In **6**, two Hamilton receptor substituents are connected to the two axial positions of $Sn^{IV}P$ through single oxygen atoms leading to octahedral coordination. As a consequence, a comparatively rigid and a spatially tight arrangement of H-bonded cyanurates and porphyrins are realized. The synthesis of **6** was accomplished by 1-ethyl-3-3-(3-dimethylaminopropyl)carbodiimide (EDC) promoted coupling of $(OH)_2Sn^{IV}$

Scheme 1. Synthesis of the Fourth Generation Depsipeptide Dendron **4**[a]

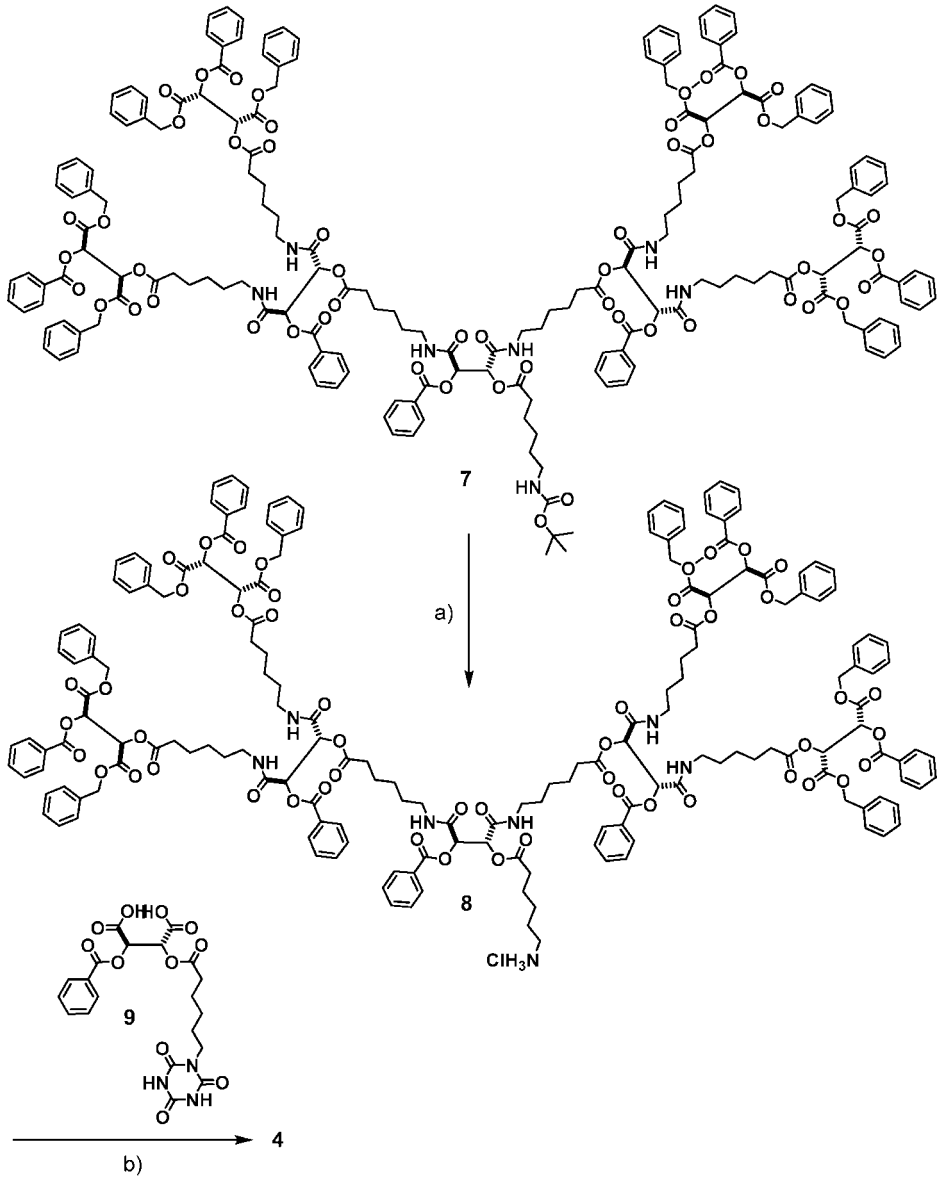

[a] (a) HCl, EtOAc, room temperature; (b) DCC, HOBt, NEt_3, CH_2Cl_2, 0°C.

Scheme 2. Final Step in the Synthesis of the Porphyrin Platform **6**

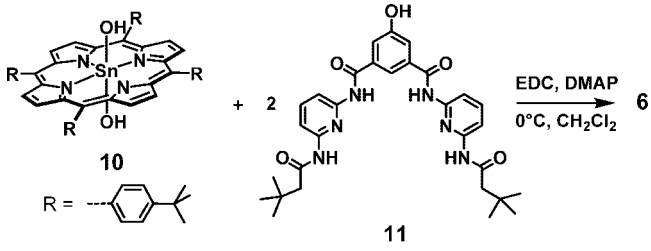

porphyrin **10**[16] with the new Hamilton receptor **11** containing a hydroxyl group at the focal point and two peripheral *neo*-pentyl substitutents to increase the overall solubility (Scheme 2). Most interestingly, this transformation of a hydroxo metalloporphyrin derivative is, to the best of our knowledge, so far not known. It should be mentioned that the conditions of the coupling reaction are extremely mild; in particular, no acid is required. We are currently exploring the carbodiimide coupling protocol for other metalloporphyrins carrying axial hydroxyl ligands.

First, the self-assembly of **6** with depsipeptide ligands **1**−**5** to yield 1:2 complexes was investigated by NMR spectroscopic assays.[17] Although chloroform was used as a solvent, to promote the self-assembly and to ensure the integrity of the hydrogen bonding, the ^{1}H NMR spectrum of **6** reveals comparatively broad and unresolved peaks. Such a trend is indicative of intermolecular aggregation instigated by hydrogen bonding, as has been noted in other Hamilton receptor systems.[10,12] However, upon successive addition of the dendritic cyanuric acid derivatives **1**−**5**, a remarkable sharpening of the signals is seen which indicates the successful forming of discrete **6:L$_n$** complex.

(16) Crossley, M. J.; Thordarson, P.; Wu, R. A.-S. *J. Chem. Soc., Perkin Trans. 1* **2001**, 2294.

(17) Chirality transfer from the depsipeptide dendrons to the porphyrins is very weak and could not be determined by CD spectroscopy.

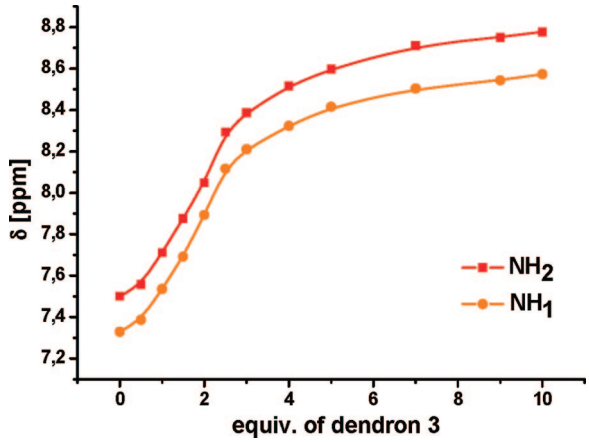

Figure 2. ^{1}H NMR titration plot of the chemical shifts of the NH_1 and NH_2 protons as a function of the amount of added dendron **3**.

Table 1. Association Constants, *R*-factor (*R*), r_{max}, and Hill coefficients for the systems **6:1$_n$**, **6:2$_n$**, **6:3$_n$**, **6:4$_n$**, and **6:5$_n$**

	log K_1 [L mol^{-1}]	log K_2 [L mol^{-1}]	*R*	r_{max}	n_H
6:1$_n$	4.45	7.89	±0.18	0.35	0.21
6:2$_n$	3.87	7.54	±0.19	0.62	0.45
6:3$_n$	3.46	7.21	±0.18	0.76	0.62
6:4$_n$	3.76	6.95	±0.50	0.50	0.33
6:5$_n$	3.73	7.46	±0.91	0.71	0.55

This observation agrees well with a characteristic low-field shift[10–12] of the NH^1 and NH^2 protons, which reflects the successive binding of the complementary ligands **1**−**5** by **6**. It is important to note that establishing the equillibria necessitated a 45 min induction period, in which the intermolecular self-assembly of **6** is overcome and the dendritic ligands are bound. The titration curves (Figure 2) are sigmoidal in shape with an inflection point at 2 equiv of added dendron.

Implicit here is a positive cooperativity in the stepwise binding process.[18] The corresponding association constants of the complexes were calculated with *Chem-Equili* and the Solov'ev method by employing the ^{1}H NMR titration data (Table 1).[19] For our systems major differences are observed for the first binding step. The smaller first and the bulky fourth generation addend lead to the highest K_1 values. In the case of the second binding step, the association constants for the second and third generation ligands are much higher compared to their first binding step. Overall the values confirm those determined for comparable systems.[10–12]

The preferred formation of **6:L$_2$** (**L** = **1**−**4**) compared to the corresponding **6:L** complexes becomes also apparent upon analyzing the distribution of the Hamilton receptor as free core (HR) and as part of the complexes **6:L$_n$** (***n*** = 1−2) as a function of added dendron equivalents (Figure 3). For example, the amount of **6:L$_2$** (**L** = **2, 3**) complexes prevails already at low concentrations of added dendrofullerene **5**. After the addition of 2 equiv of dendron **2** and **3**, respectively, the amount of **6:L$_2$** complexes ranges between 50 and 70%. On the other hand the formation of **6:L$_2$** complexes involving **1** and **4** is much less pronounced (Figure 3). The **6:L$_2$** fraction does not become predominant until 4 equiv or more of the ligands are added.

The Scatchard plots give rise to a convex shape and are indicative of pronounced positive cooperativity during the formation of the complexes (Figure 4).[20] In contrast a concave shape would indicate negative cooperativity, and a straight line would suggest no cooperativity at all. To this end, the most straightforward presentation of the cooperativity phenomena is based on determining the occupancy *r*. In particular, the maxima of the Scatchard plot (r_{max}) allow the determination of the Hill coefficients (n_H).[21] The amount of cooperativity is directly correlated to the value of n_H. The largest n_H values are found for the third generation and the lowest n_H for the first generation system.

The observed association properties of the porphyrin **6** with the dendritic ligands **1**−**4** can be explained when looking closely at the intermolecular interactions of the porphyrin **6**. In a nonpolar solvent like toluene or chloroform the Hamilton receptors of **6** tend to self-aggregate via hydrogen bonding. The first binding step of a dendritic ligand leads to a weakening of this intermolecular self-assembly, because the solubility of the newly formed **6:L** complex is improved by the bulky dendritic unit. The higher solubility causes a higher accessibility for the second Hamilton receptor which leads to a higher second association constant. This behavior explains the observed association phenomena such as the positive cooperativity of the second binding step. In this case the highest positive cooperativity was found for the third-generation dendrons. Very bulky ligands, on the other hand, disfavor this subsequent binding step because of their sterical demand. The most pronounced positive cooperativity is achieved when these factors are well balanced.

Molecular modeling suggests for **6** a rigid arrangement with an almost octahedral coordination around the tin atom leading to an in-plane *all-trans* configuration of both receptor units (Figure 5). Thus, initially both dendrimer binding sites are considered to be equal.

Rotational degrees of freedom of the sp^3-carbon network in **2**, **3**, and **4** lead to many possible rotamers and a large conformational space. In fact, the potential energy surface is very complex exhibiting several local energy minima, which are separated from the global energy minimum by very low energy barriers. However, considerable $\pi-\pi$ interactions between the phenyl end groups, as they have already been found for **2** and **3** in the gas phase, enable a rather compact arrangement of the dendrons with accessible cyanuric acid binding sites. To assess the hydrogen bonding interactions in the Hamilton receptor units, we have optimized the porphyrin unit **6** in the presence of **2** lacking the phenyl rings. The resulting geometries reflect the strength of the directional six-point binding motif of the cyanuric acid moieties when interacting with the Hamilton receptor units. In all cases, hydrogen-bonding distances on the order of 2.0 to 2.2 Å (Figure 6) confirm favorable interactions between the porphyrin unit and the dendrimer binding site.

Furthermore, we employed molecular mechanics calculations to determine the global minimum and to explore the conformational space of the complexes between the acceptor units

(18) Schneider, H.-J.; Yatsimirsky, A. *Principles and Methods in Supramolecular Chemistry*; Wiley-VCH: Chichester, 2000.
(19) (a) Solov'ev, V. P.; Baulin, V. E.; Strahova, N. N.; Kazachenko, V. P.; Belsky, V. K.; Varnek, A. A.; Volkova, T. A.; Wipff, G. *J. Chem. Soc., Perkin Trans. 2* **1998**, 1489. (b) Solov'ev, V. P.; Vnuk, E. A.; Strakhova, N. N.; Reavsky, O. A.; VINITI, Moscow, 1991.
(20) (a) Badjić, J. D.; Nelson, A.; Cantrill, S. J.; Turnbull, W. B.; Stoddart, J. F. *Acc. Chem. Res.* **2005**, *38*, 723. (b) Ercolani, G. *J. Am. Chem. Soc.* **2003**, *125*, 16097. (c) Perlmutter-Hayman, B. *Acc. Chem. Res.* **1986**, *19*, 90. (d) Scatchard, G. *Ann. N.Y. Acad. Sci.* **1949**, *51*, 660.
(21) (a) Hill, A. V. *Biochem. J.* **1913**, *7*, 471. (b) Hill, A. V. *J. Physiol. (London)* **1910**, *40*, 4.

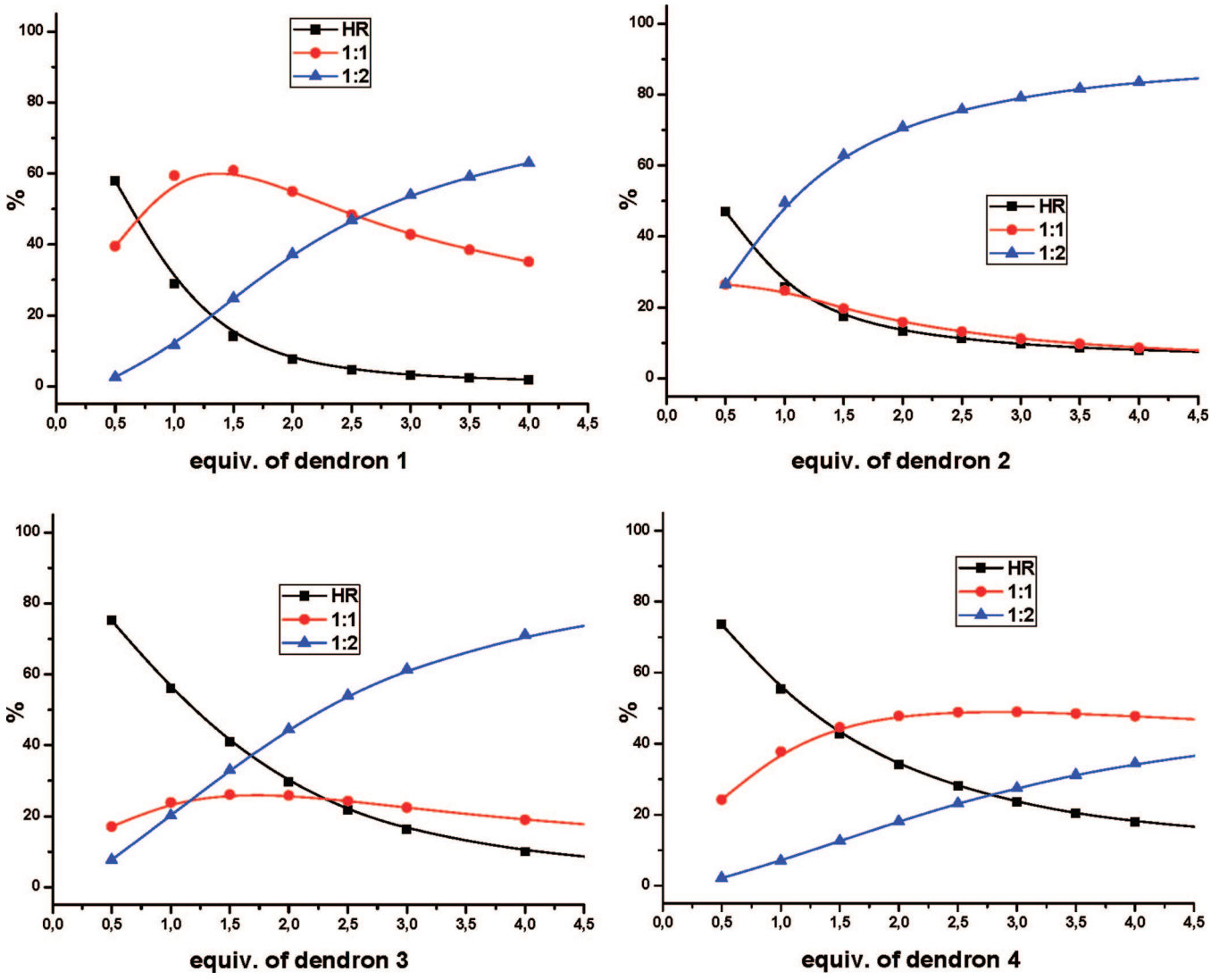

Figure 3. Distribution in percent of the porphyrin as free core (HR) and within the complexes **6**:$\mathbf{L}_n$ (n = 1−2) as a function of the amount of added dendrons **1**−**4**.

(**2**, **3**, **4**) and the receptor (**6**). We investigated the three different 1:1 and 2:1 complexes of the cyanuric acid derivatives with **6**. We note the high flexibility of the sp^3-carbon network in **2**, **3**, and **4**, and as a direct consequence many possible low-energy conformations, with an energy difference of less than 2 kcal/mol relative to each other, emerge. In order to preserve the hydrogen-bonding interactions we have constrained the structure of the binding site and carefully decreased the constrain energy to maintain the binding properties of the dendrimers and SnP **6**.

All calculations revealed a fairly rigid arrangement between the porphyrins and the H-bonded cyanurates. Also important is that the porphyrin framework preserves its planarity throughout the entire simulation and is independent of the size of the dendrimer. In the 1:1 complexes rotational and translational modes of the receptor units, which are involved in binding of the cyanuric acid derivatives, are almost completely restrained, whereas the free accessible binding sites exhibit considerable flexibility during the entire simulation. On one hand, this implies stable hydrogen bonding between the cyanurates and the receptors in the 1:1 complexes. On the other hand, complexation of only one ligand does not influence the conformation of the second Hamilton receptor, namely all-cis in favor of all-trans. Still a notable weakening of the intermolecular hydrogen bonds is discernible during the complexation of the first ligand. This trend is, however, dependent on the dendron size. In all 1:1 complexes significant $\pi-\pi$ interactions between **6** and the first ligand are observed with increasing dendron generation. In turn, the ligand adopts a very compact conformation, in which the phenyl units will interact with the porphyrin π-system due to the closer contacts. As a consequence, enhanced shielding of the porphyrin framework by the bulky ligands was noticed, and hence, the unoccupied Hamilton receptor binding site becomes more accessible toward a second ligand with increasing size of the dendron. These interactions prevent a reaggregation via the hydrogen bonds of **6**. Moreover, steric hindrance forces the second receptor into a cis−cis planar configuration, which (i) makes it more accessible, (ii) is most favorable for ligand binding, and (iii) propagates favorable $\pi-\pi$ interactions between the phenyl units of the receptor (Figure 7).

In summary, MD simulations show strong interactions between the porphyrin framework and the dendritic ligands in the 1:1 complexes. These interactions tend to increase with increasing size of the ligand and facilitate the second binding step due to deaggregation of the intermolecular hydrogen bond network of **6**. As a consequence, the second Hamilton receptor

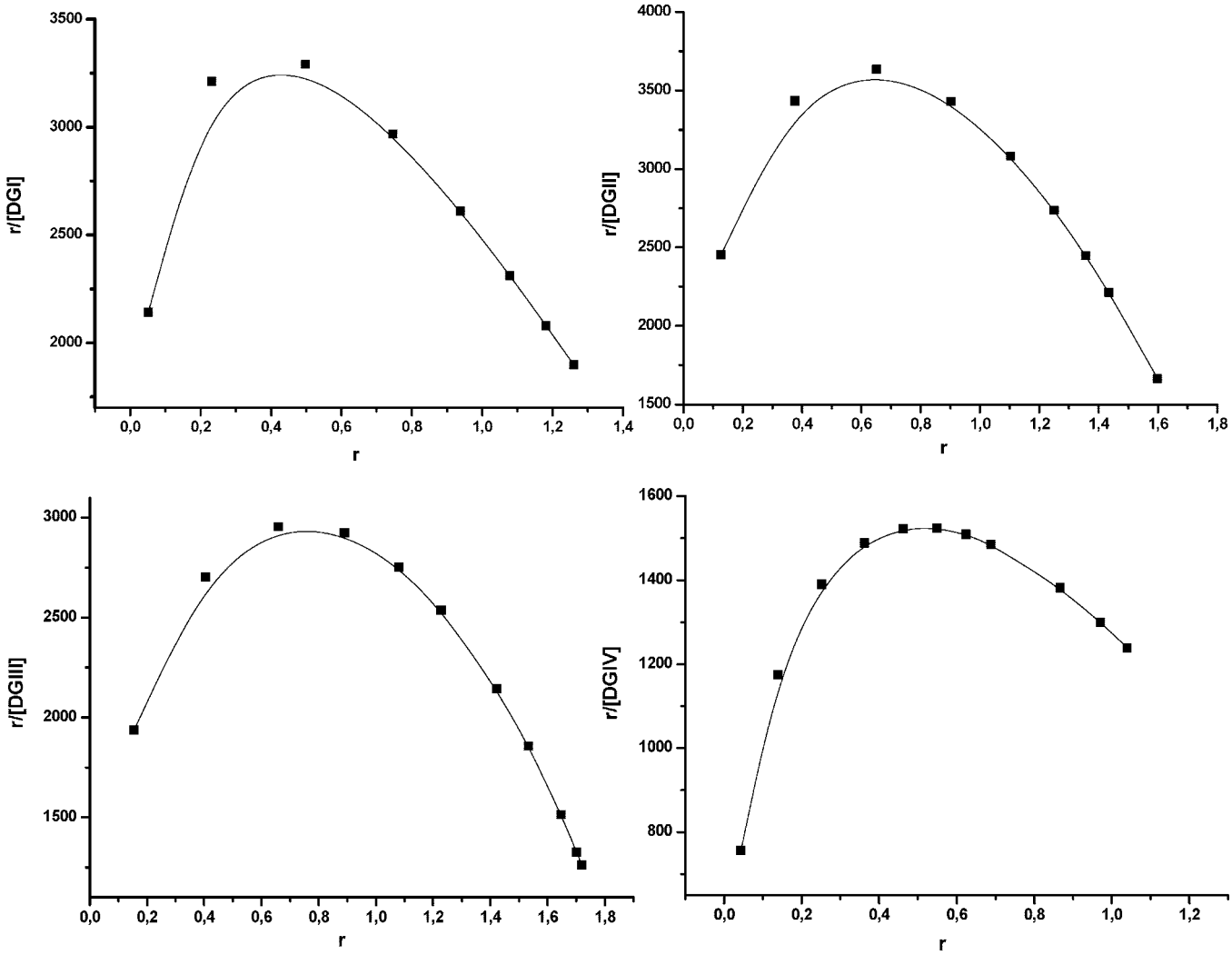

Figure 4. Scatchard plots for the systems **6**:L_2 (L = **1**−**4**).

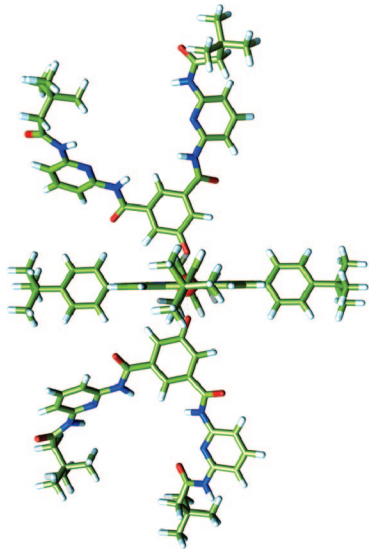

Figure 5. AM1 optimized structure of **6**.

becomes more accessible to the second ligand. A sterically more demanding ligand prevents reaggregation of the 1:1 complex. However, with increasing dendron generation, the positive cooperativity tends to decrease. The second ligand in **6**:$\mathbf{4}_2$ encounters significant steric hindrance during the second binding step, which ratifies the unexpected decrease of the binding constant (Figure 8).

Support for the dynamic character of the equilibrium, that is, forming the 1:2 complexes of **6** and the depsipeptide ligands **1**−**5**, came from temperature dependent NMR measurements. Whereas at room temperature the NH protons of both species, bound and free ligand, give rise to a broad signal at 11.5 ppm, two signals appear upon cooling down to −30 °C at 9 and 13.5 ppm for the free and the bound dendrons, respectively.[10]

Porphyrin **6** has emerged as a versatile platform that enables, through exchanging **4** and **5**, the reversible interconversion between **6**:$\mathbf{4}_2$ and **6**:$\mathbf{5}_2$. Qualitative support for such a dynamic exchange came from titration assays, in which complex **6**:$\mathbf{4}_2$ was probed in the absence and presence of variable concentrations of **5**. Figure 9 documents that an incremental addition of **5** to **6**:$\mathbf{4}_2$ leads to a notable quenching of the fluorescence, which was indeed fully reverted into the strongly fluorescing **6**:$\mathbf{4}_2$ upon adding an excess of **4**.

A series of photophysical measurements provided mechanistic insights into the aforementioned excited-state interactions, namely, the reversible replacement of **4** (i.e., **6**:$\mathbf{4}_2$) with **5** (i.e., **6**:$\mathbf{5}_2$) and vice versa. The lack of considerably photoactivity and redox activity of **4** evokes in **6**:$\mathbf{4}_2$ no appreciable trends. In fact, the fluorescing features of **6**:$\mathbf{4}_2$ are virtually identical to those

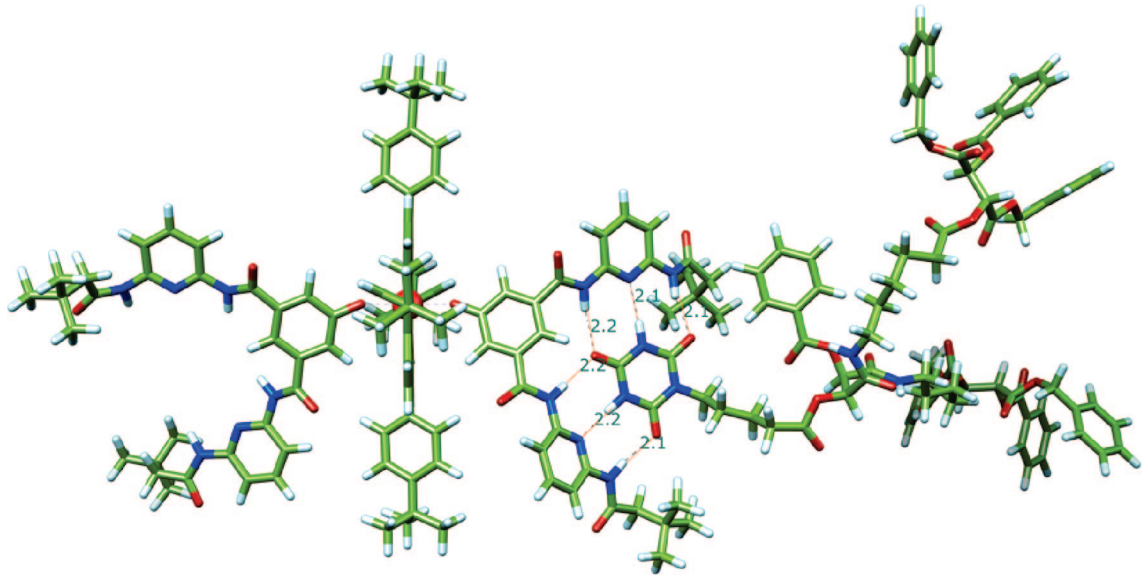

Figure 6. AM1 optimized structure of **6:2** representing the hydrogen-bonding interactions and the bond distance in Å.

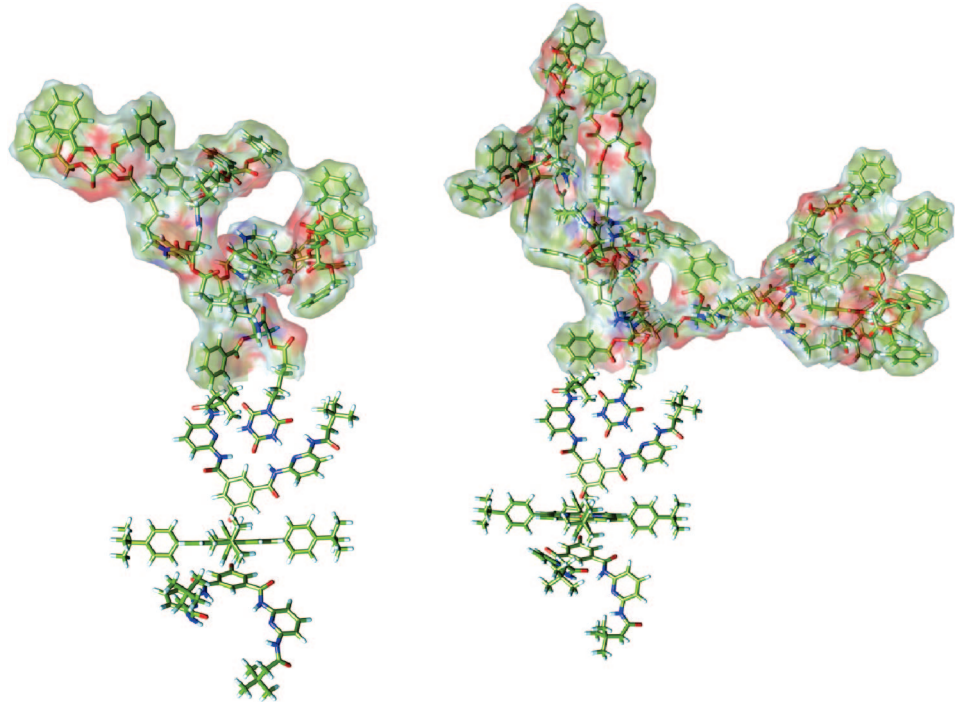

Figure 7. Minimum-energy conformations of the 1:1 complexes **6:3** and **6:4** visualizing the flexibility of the sp^3-carbon network of the ligands; the surface represents the local-energy-minima conformational space.

seen for **6** in the absence of **4**; see Figure S1. To name a few photophysical features: fluorescence quantum yields and lifetimes of 0.003 and 0.3 ns, respectively. Adding **5**, however, results in a substantial quenching of the porphyrin centered fluorescence maxima at 610 and 665 nm. As illustrated in Figure 10, the quenching is exponential and depends exclusively on the added concentration of **5**, which points to the successful formation of **6:5$_2$**. From the underlying nonlinear relationship we determined the association constants for binding 1 and, subsequently, 2 equiv of **5**. Reassuringly, both K values, log K_1 (i.e., 3.6 M^{-1}) and log K_2 (i.e., 6.9 M^{-1}), are in excellent agreement with those determined in the NMR titrations. When reversing the titration, that is, adding variable concentrations of **4** to **6:5$_2$**, a gradual reactivation of the fluorescence is noted, Figure S2. From the underlying fluorescence intensity versus **4** concentration relationship, log K_1 (i.e., 2.3 M^{-1}) and log K_2 (i.e., 5.1 M^{-1}) were derived.

Notably, at the end point of the titration (i.e., **6:5$_2$**) the porphyrin fluorescence is nearly quantitatively quenched. Instead, a fluorescence pattern (i.e., *0−0 emission around 700 nm) evolved that is reminiscent of that of **5**.[22] Please note that this happens although the porphyrin component in **6:5$_2$** is exclusively excited. To shed light onto the mechanism by which the fullerene fluorescence is generated, an excitation spectrum was taken. Importantly, the excitation spectrum is an exact match of the ground-state absorption of the porphyrin with maxima at

(22) Guldi, D. M.; Prato, M. *Acc. Chem. Res.* **2000**, *33*, 695.

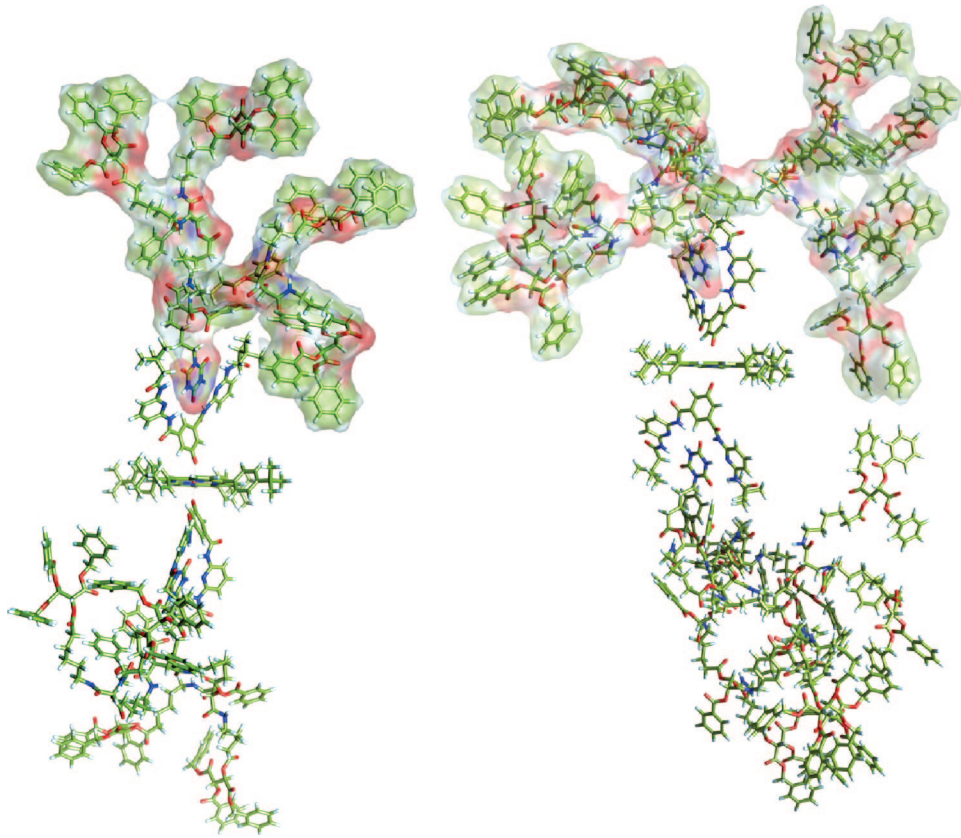

Figure 8. Structure of **6:3$_2$** and **6:4$_2$** resulting from a 50 ps quench molecular dynamics simulation *in vacuo* using the COMPASS force field parameters after prior conjugate-gradient minimizations; the surface represents the local-energy-minima conformational space.

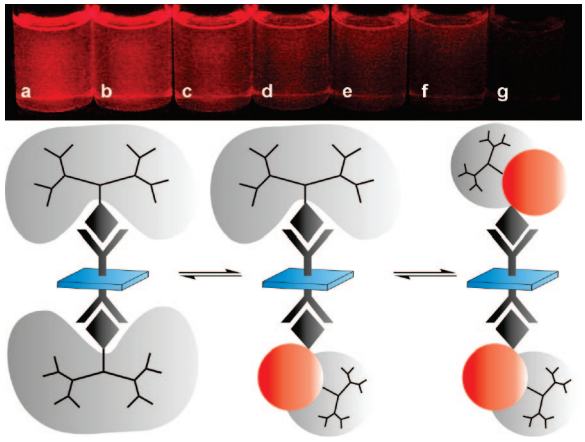

Figure 9. (Upper part) Qualitative fluorescence quenching of **6** upon variable additions of **5** to **6:4$_2$**: (a) 0 equiv of **5**, (b) 0.5 equiv of **5**, (c) 1 equiv of **5**, (d) 1.5 equiv of **5**, (e) 2 equiv of **5**, (f) 4 equiv of **5**, (g) 6 equiv of **5**. (Lower part) Schematic representation of the ligand exchange reaction between **6:4$_2$** and **6:5$_2$**.

430, 560, and 600 nm (Figure S3). This leads us to hypothesize that a thermodynamically driven transduction of singlet excited-state energy from the porphyrin (1.98 eV) to the fullerene (1.79 eV) must govern the photoactivity of **6:5$_2$**.

Conclusive information about the nature of the interactions came from transient absorption measurements, femtosecond and nanosecond, with **6** in the absence and presence of variable concentrations of **4** and **5** following 420 nm excitation. Following the time evolution of the characteristic singlet excited-state features of **6**, for instance, is a convenient mode to identify spectral features of the resulting photoproducts and to determine absolute rate constants for the intramolecular decay.

Up front, the excited-state properties of **6** shall be discussed, since they emerge as important reference points for the interpretation of the features expected in **6:4$_2$** and **6:5$_2$**. Figure 11 illustrates that the differential spectrum recorded immediately after the 420 nm excitation of **6** reveals the instantaneous (i.e., $>10^{12}$ s^{-1}) formation of the singlet excited state, for which the following features have been gathered: maxima at 455 and 800 nm as well as minima at 560 and 603 nm. The triplet excited-state features, on the other hand, include maxima at 500, 582, and 640 nm.[23] The interplay between both excited states is documented by (i) the occurrence of an isosbestic point at 480 nm and (ii) the close resemblance of the decay and formation of the singlet and triplet excited-state features, respectively (1.3×10^9 s^{-1}).

For **6:4$_2$**, the transient changes, spectroscopically and kinetically, that develop are dominated in the visible and in the near-infrared by features that correlate nicely with those seen for **6**. This, again, confirms the lack of photoactivity and redox activity of **4**.

Regarding the femtosecond transient absorption measurements of **6:5$_2$** (Figure 12), immediately, after the laser excitation, the strong singlet−singlet absorptions of **6** start to grow in with about $>10^{12}$ s^{-1}, maxima at 455 and 800 nm as well as minima at 560 and 603 nm. This confirms that, despite the presence of **5**, the porphyrin singlet excited state is successfully formed. Instead of seeing, however, the slow ISC dynamics the

(23) Complementary nanosecond experiments corroborated the formation of the oxygen sensitive SnP triplet excited state (Figure S4).

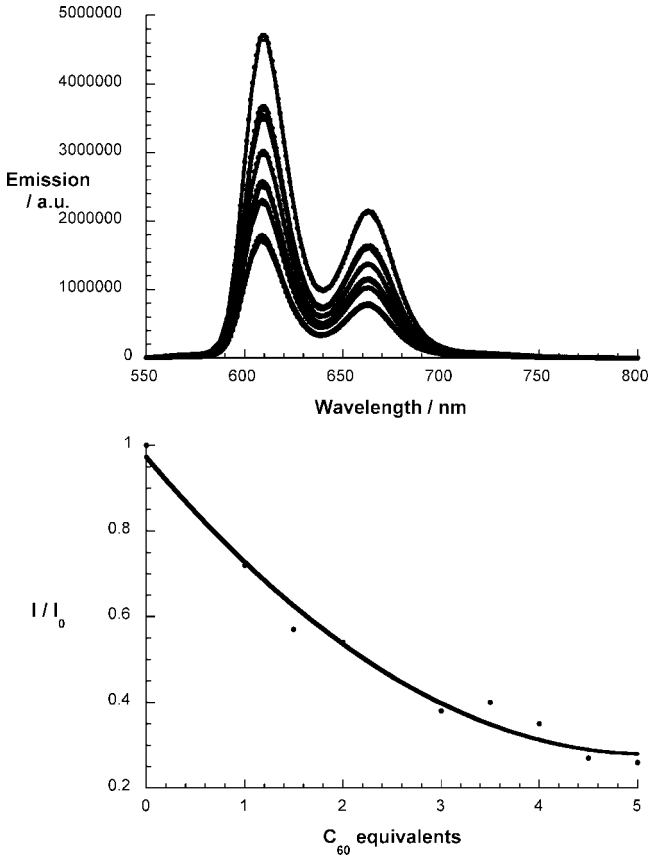

Figure 10. (Upper part) Room temperature fluorescence spectra of **6** (2.5×10^{-5} M) in the presence of variable concentrations of **5** (i.e., 0, 1.25×10^{-5}, 2.5×10^{-5}, 3.75×10^{-5}, 5.0×10^{-5}, 6.25×10^{-5}, 7.5×10^{-5}, 8.75×10^{-5}, 1.0×10^{-4}, 1.125×10^{-4}, and 1.25×10^{-4} M) upon 410 nm excitation, after correction for competitive ground absorption. (Lower part) I/I_0 versus **5** relationship used to determine the association constant.

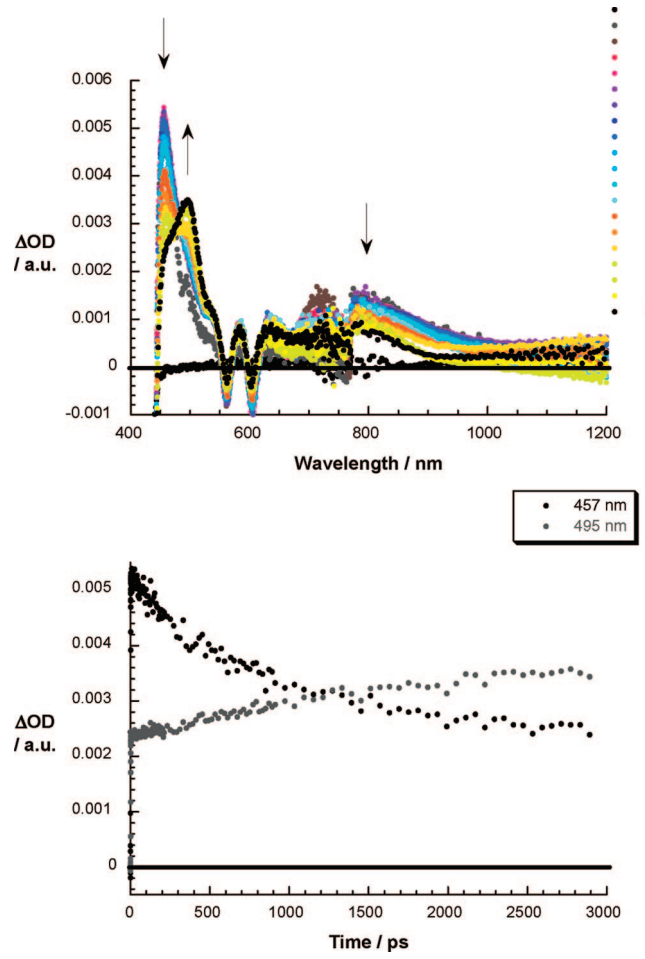

Figure 11. (Upper part) Differential absorption spectra (visible and near-infrared) obtained upon femtosecond flash photolysis (420 nm) of **6** in toluene with several time delays between 0 and 3000 ps at room temperature; see color code for details. Arrows illustrate the changes. (Lower part) Time−absorption profile of the spectra shown above at 457 nm (black spectrum) and 495 nm (gray spectrum), reflecting the singlet excited-state decay and triplet excited-state formation, respectively.

singlet−singlet absorptions decay in **6:5$_2$** with accelerated dynamics. To this end we noted that with increasing time delay the porphyrin singlet excited-state features change to a transient that bears no resemblance with its triplet excited state at 497, 582, and 640 nm, the product of the intersystem crossing seen in **6**. Instead near-infrared features develop that reveal a maximum at around 900 nm. Unequivocally, this signature has been established as an attribute of the singlet excited state of **5**.[22] This finding supports formation of one transient species (i.e., fullerene singlet excited state) at the expense of the other transient species (i.e., porphyrin singlet excited state). Notably, the porphyrin decay and the fullerene formation dynamics, 2.8×10^{10} s^{-1}, resemble each other.

Analysis of the newly formed fullerene singlet excited-state features confirms the metastability in **6:5$_2$**. The lifetime is 1.3 ns (7.7×10^8 s^{-1}) identical to what has been derived for the intersystem crossing in **5** to afford accordingly the triplet manifold ($E_{\text{Triplet}} = 1.5$ eV). Moreover, the transient absorption features exhibit at the conclusion of this decay a maximum at 720 nm, which is a known fingerprint for the triplet excited state of C_{60}.[22,24]

In line with the proposed energy transfer mechanism the differential absorption changes, recorded immediately after a 8 ns pulse with **6:5$_2$**, showed the same spectral features of the fullerene triplet excited state as observed at the end of the femtosecond experiments. The spectral attributes of the fullerene triplet excited state, precisely, two maxima located at 360 and 720 nm, were observed. Thus, our analysis clearly shows the photosensitization effect of the porphyrin chromophores, acting as an antenna system and transmitting its excited energy to the noncovalently associated fullerene moieties.

For determining the fullerene triplet quantum yields in **6:5$_2$** we utilized the quantitative conversion of the triplet excited states of the porphyrin (0.78) and fullerene (i.e., 0.98) fragments into singlet oxygen. By analyzing the singlet oxygen emission at 1275 nm (see Figure 13), we derived a quantum yield of 0.84.

Conclusions

To summarize, we have successfully demonstrated the hierarchical integration of a porphyrin core as well as chromophoric and/or nonchromophoric dendrons through means of hydrogen bonding. Insights into the nature of the interactions came from diverse titration and photophysical experiments, which revealed the dynamic character of the self-assembly in the 1:1 and 1:2 complexes of porphyrin **6** and the dendrons.

In line with the modeling and calculations, titration and photophysical experiments shed light onto the interactions,

(24) Addition of variable amounts of the dendron, to yield **6:4$_2$**, leads to no notable changes.

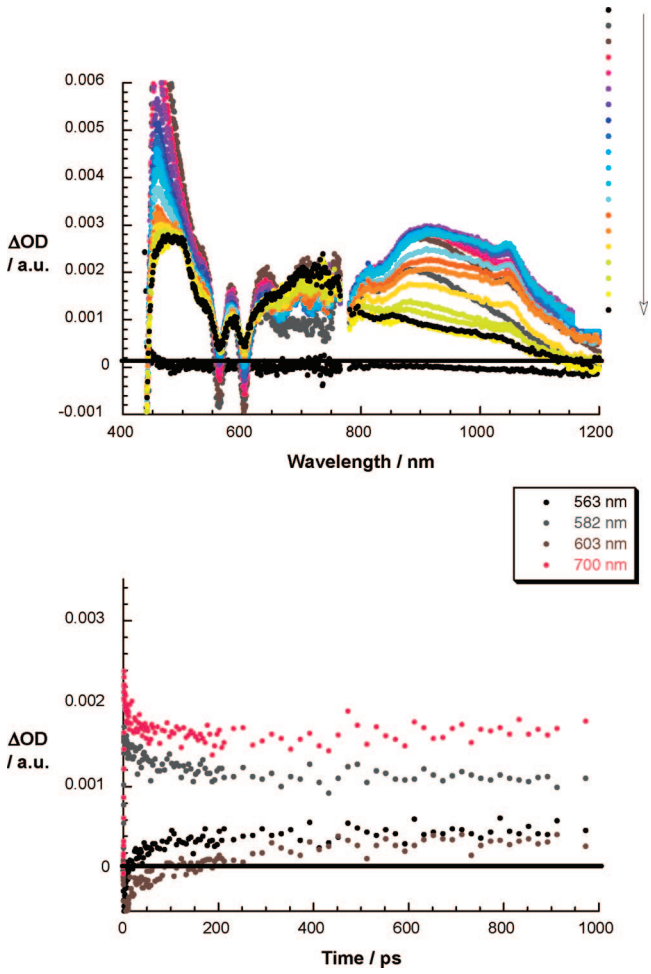

Figure 12. (Upper part) Differential absorption spectra (visible and near-infrared) obtained upon femtosecond flash photolysis (420 nm) of **6:5**$_2$ in toluene with several time delays between 0 and 3000 ps at room temperature; see color code for details. (Lower part) Time−absorption profile of the spectra shown above at 563, 582, 603, and 700 nm, reflecting the energy transfer process.

namely, the reversibility and the dynamic equilibrium of the complexation behavior. Furthermore, the examination of excited-state characteristics revealed significant energy transfer properties of these complexes upon photoexcitation. Implicit is a mediation of singlet excited-state energy driven by noncovalent hydrogen-bonding interactions. To this end, hydrogen bonding interactions enable the facile exchange/variation of the binding motifs/binding partner and, in turn, the flexible tuning of

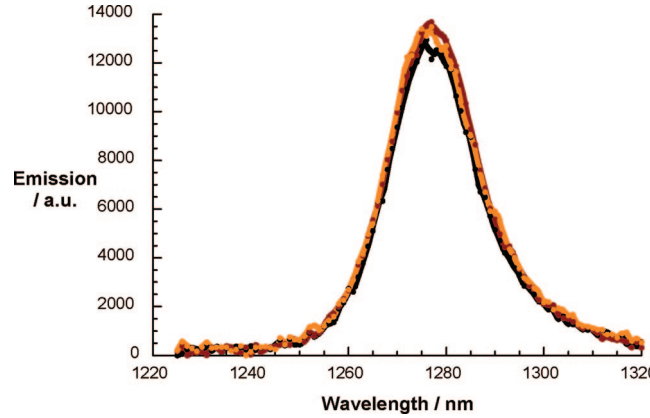

Figure 13. Singlet oxygen emission, measured at 1275 nm, for **5** (red spectrum), **6** (black spectrum), and **6:5**$_2$ (orange spectrum) in toluene upon 355 nm excitation.

distance, orientation, and energy gap, to name a few important variables. Cascades of energy transfer reactions, along well devised energy gradients, are conceivable, when, for example, different generations of dendrimers would be implemented.

Nevertheless, additional complexation experiments with, for instance, branching units are needed to understand all the details and facets of the self-assembly process. Important for this understanding will be the development of a supramolecular toolbox—with the presented **6:L**$_n$ complexes considered as one of the simplest systems thereof—that includes porphyrins, fullerenes, dendrimers, and other functional molecules to construct larger and more variable assemblies. An important aspect will focus on surrounding the porphyrin core with a more compact shell of higher generation dendrimers. Obviously, this would impact ligand exchange reactions.

Acknowledgment. This work was supported by the Deutsche Forschungsgemeinschaft DFG (SFB 583: Redoxaktive Metallkomplexe - Reaktivitätssteuerung durch molekulare Architektur) and by the Cluster of Excellence: Engineering of Advanced Materials.

Supporting Information Available: Photophysical data, containing room temperature fluorescence spectra of **6** in the presence of **4** and **5** (S1, S2), excitation spectrum of the **6:5**$_2$ complex (S3), and differential absorption spectra of **6:4**$_2$ (S4). Experimental details, including synthesis, characterization, and molecular modeling. This material is available free of charge via the Internet at http://pubs.acs.org.

JA8018065